



Research article

Development of a high temperature printable composite for microwave absorption applications

Leticia Martinez^{1,2}, Den Palessonga¹, Philippe Roquefort³, Alexis Chevalier¹, Azar Maalouf¹, Julien Ville³ and Vincent Laur^{1,*}

¹ Lab-STICC, University of Brest, France

² Universidad Rey Juan Carlos, Spain

³ IRDL, University of Brest, France

* **Correspondence:** Email: vincent.laur@univ-brest.fr.

Abstract: This study deals with the development of a printable composite material based on a polyphenylene sulfide (PPS) matrix and carbonyl iron (Fe) particles, with controlled electromagnetic performance. More specifically, materials were simultaneously melt mixed and shaped under the form of filament with a diameter suitable for Fused Deposition Modeling. After reminding the potentialities of the printable PPS matrix, especially in terms of temperature resistance, microwave characterizations were performed on toroidal samples. The measured electromagnetic properties were compatible with absorption applications and compared to those of a commercial iron-filled PolyLactic Acid (PLA). Rectangular waveguide microwave loads were designed and fabricated by Fused Deposition Modeling with both materials. The PPS-Fe load has a volume that is 7 times lower than the PLA-Fe load due to a higher permittivity-permeability product and losses. Heat treatments demonstrated that no degradation is observed for the PPS-Fe load up to 180 °C while the PLA-Fe load is totally melted at 150 °C. In the same time, it was observed that the maximum power supported by the PPS-Fe load is three times higher than the one supported by the PLA-Fe load. Finally, the temperature stability of the electromagnetic response of the PPS-Fe composite was demonstrated by measurements in the –70 °C to 140 °C temperature range. This new high temperature printable composite paves the way to the development of efficient, low-cost, low-weight, power and temperature stable absorbers for microwave applications.

Keywords: 3D printed load; fused deposition modeling; microwave load; polyphenylene sulfide (PPS); printable composite material; polylactic acid (PLA)

1. Introduction

Additive technologies are currently disrupting many areas, including microwave electronics. They make it possible to produce objects of complex shapes, which cannot be produced by standard methods. Among the various methods available, Fused Deposition Modeling (FDM) is a low-cost shaping technique consisting of layer-by-layer deposition of a molten polymer. This technique requires a fine optimization of the different parameters in order to ensure the surface quality and the dimensional accuracy of the printed parts as well as the adhesion between the first printed layer and the printing bed so that a lot of studies deal with this issue [1-3].

Many demonstrators (filters, antennas, etc.) have been made by this technique in recent years [4,5]. Moreover, this technique makes it possible to shape composite materials whose electromagnetic (EM) properties can be compatible with microwave absorption applications. Thus, it has been demonstrated that 3D printed efficient microwave absorbers can be designed using composites in a single material [6–9] or multi-materials [10] approach. Rectangular waveguide loads can also be realized by 3D printing with high absorption levels at reduced cost and mass [11,12]. However, these demonstrations were made from commercial materials diverted from their initial applications but not having exactly the desired EM properties (permittivity, permeability, loss tangent). As a result, dedicated printable materials must be developed [13].

One of the main limitations of the application of this technology concerns the maximum service temperature of polymer matrices that are used in 3D printing technology. As an example, the glass transition temperature is around 50–60 °C for polylactic acid (PLA) [14] and about 100 °C for acrylonitrile butadiene styrene (ABS) which are the most used matrices in FDM [15]. Such limit-temperatures are not compatible with the military, aeronautical or space domains that require continuous temperature resistance up to 150 °C [16].

Thus, new printable technical materials have been developed recently. Polyetherimides (PEI) [17], also known as Ultem, polyetheretherketones (PEEK) [18] or printable phenylene polysulfides (PPS) now appear as suitable solutions for producing thermally stable components because of their high continuous working temperatures. These thermoplastics can also serve as a matrix for the preparation of composites.

In this study, a PPS matrix, resistant to high temperatures and therefore high-power levels, is proposed to be used to develop radar absorbing materials. The development of a composite based on PPS matrix reinforced with carbonyl iron (Fe) particles will be described. Then, this material was used to fabricate a microwave load whose performance as a function of temperature and power level was evaluated.

2. Elaboration of the composite

The material selected for this study is a PPS (nPower supplied by 3NTR). The EM properties of the PPS were measured using an X-band (8–12 GHz) rectangular waveguide characterization method detailed in [8]. This polymer has a non-dispersive permittivity close to 3 in the measured frequency band. Its dielectric losses are 7.4×10^{-3} between 8 and 12 GHz. A previous detailed study on the potentialities of the printable PPS for microwave applications, including temperature resistance, has clearly shown no degradation of PPS-based devices up to 200 °C [19].

Thus, a composite based on PPS matrix with a volume fraction of Fe particles (FE006041

supplied by Goodfellow) of 20% was prepared by simultaneous melt mixing, without using any dispersant to pretreat Fe particles, using a DSM Xplore twin screw extruder at a temperature of 330 °C and a screw speed of 50 rpm. The mixing time didn't exceed 90 s. It is worth pointing out that Fe particles volume fraction of 20% is a good compromise between mechanical strength and EM properties of the composite [13]. Besides, the microstructure of the composite shows the presence of spherical Fe particles with a diameter between 6 and 8 μm, embedded in the thermoplastic matrix, without any aggregate, as shown on scanning electron microscopy (SEM) image (Figure 1). Indeed, if we consider that the average shear rate, during mixing, is equal to 785 s⁻¹, estimated from the technical data, it is possible, according to the equation of Schmolukoski, to estimate a frequency of 400 particles collisions per second for Fe particles volume fraction of 20%. Consequently, the increase of Fe content leads to an increase of the number of collisions and might explain that the break-up of the few largest particles is easier.

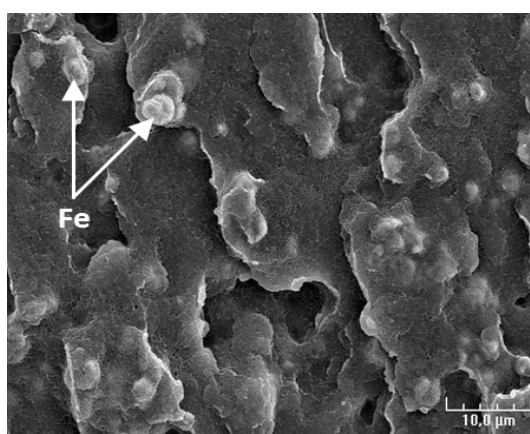


Figure 1. SEM image of a PPS-Fe 80/20 vol% composite.

After melt mixing, all samples were pelletized and processed under filament with a diameter close to 3 mm using a single-screw Filabot Extruder EX2 conveyor at a temperature close to the melting temperature of the PPS (283 °C). An iron-filled composite PLA-Fe (supplied by Proto-pasta under the form of filament) has been selected to compare its EM properties with those of the PPS-Fe composite. The density of these filaments was measured. The measured densities were 1.88 g·cm⁻³ and 2.37 g·cm⁻³ for the PLA-Fe and PPS-Fe filaments, respectively. This difference of densities seems to be mainly due to a higher iron filling ratio in the lab-made PPS-Fe composite.

3. Microwave characterization

All the filaments of the study were shaped using a 3NTR A2V4 3D printer. Printed objects (samples for the characterization and components) were made with layer thicknesses of 200 μm under temperature conditions given in Table 1. Printing parameters were chosen in order to minimize the samples porosity. The mass and volume of the different printed samples were then measured in order to evaluate the densities of the printed objects. Densities of 1.68 g·cm⁻³ and 1.89 g·cm⁻³ were extracted from the measurements for PLA-Fe-based samples and PPS-Fe-based samples, respectively. One should note that these decreases of densities correspond to porosity of 20.1% in the PPS-Fe

samples and of 10.3% in the PLA-Fe samples. The higher porosity in the PPS-Fe samples can be explained by the higher variation of the lab-made-filament diameter than can induce a variation of the material flow during the printing process.

Samples with toroidal geometry were fabricated in order to allow an extraction of EM properties (complex permittivity and permeability) using a standard APC7 coaxial line method.

Table 1. Temperatures used during the printing process.

Material	Bed temp. (°C)	Chamber temp. (°C)	Nozzle temp. (°C)
PLA-Fe	60	60	200
PSS-Fe	110	75	330

Figure 2 shows measured EM properties of PLA-Fe and PPS-Fe composites in the 8–12 GHz band. The composite based on PPS matrix with Fe particles has a constant permittivity $\epsilon_r = 6.11$ associated with low dielectric losses $\tan\delta_\epsilon = 0.018$. The permeability decreases slightly over the frequency band under study with an average value close to 1.27. At the frequency of 8 GHz, its magnetic losses are relatively high $\tan\delta_\mu = 0.32$ and compatible with EM absorption applications. The iron-filled PLA has the following electromagnetic properties: $\epsilon_r = 4.17$, $\tan\delta_\epsilon = 0.012$, $\mu_r = 0.88$ and $\tan\delta_\mu = 0.14$ at 8 GHz. One should suppose that iron filling ratio in this commercial composite is lower than the one developed in our laboratory in accordance with the higher density of our composite; moreover, iron particles could exhibit different magnetic properties. However, these EM properties remain compatible with the design of a microwave load.

Once the commercial PLA-Fe composite and the lab-made PPS-Fe composite have been characterized, two loads with similar absorption characteristics were designed.

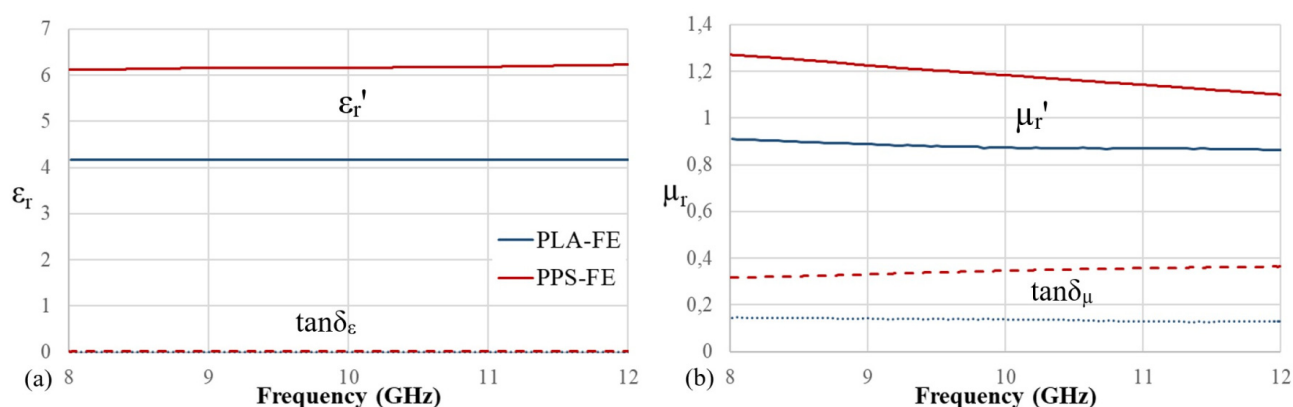


Figure 2. (a) Permittivity and (b) permeability of PPS-Fe and PLA-Fe printed composites in the 8–12 GHz band.

4. Microwave load realization and measurements

Two rectangular waveguide (standard WR-90 8–12 GHz) loads were designed to provide quite similar reflection coefficients for the two composites in the frequency band of interest. Devices were designed by using a commercial 3-D electromagnetic software (Ansys HFSS) based on a finite-element method. These simulations took into account the dispersion of PLA-Fe and PSS-Fe

electromagnetic properties (permittivity and permeability). The selected topology is a simple wedge having a base length l_b , a pyramid length l_p and a width w_p (Figure 3). Table 2 shows the dimensions for each material. As the EM properties of the two filaments are different, the load made with the PLA-based composite is larger and longer than the one made with the PPS-based composite. Simulations predict a minimum reflection of -13.6 dB at 9.19 GHz for the PLA-Fe-based load and of -18 dB at 8.57 GHz for the PPS-Fe-based load.

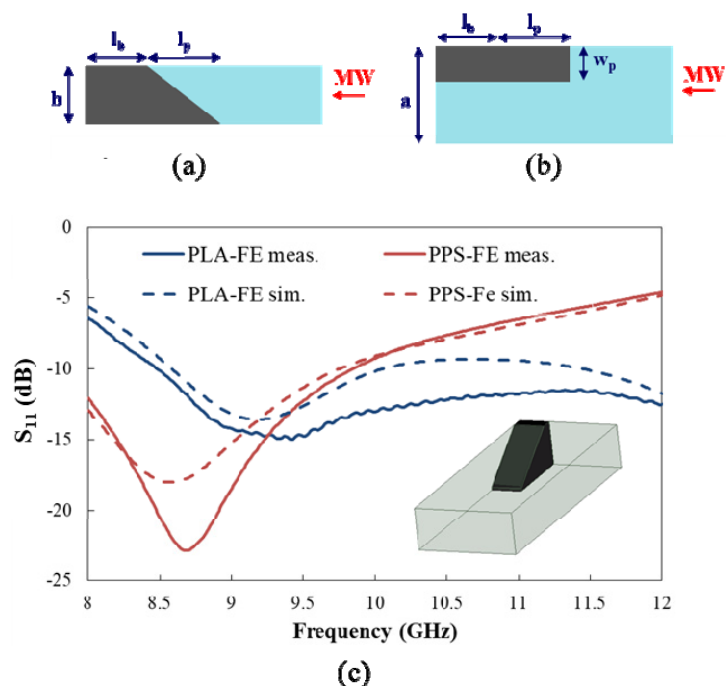


Figure 3. (a) Side and (b) top view of the load, (c) Comparison between measured and simulated reflection coefficient of the two loads printed with PPS-Fe and PLA-Fe between 8 and 12 GHz.

Table 2. Load dimensions (mm).

Material	l_b	l_p	w_p
PLA-Fe	5	15	20
PSS-Fe	3	10	5

The components were printed with the same parameters used to print the characterization samples. For the measurement, the load was placed in a short-circuited waveguide. Thru-Reflect-Line (TRL) calibration was performed to overcome the influence of cables and waveguide/coaxial line transitions. The measurement of the reflection coefficient demonstrates a quite good agreement with simulations in both cases and thus confirms the validity of the EM properties of these materials and the control of the fabrication process (Figure 3). The PPS-Fe load shows a maximum absorption of 22.9 dB at 8.68 GHz and the PLA-Fe load a maximum of 15 dB at 9.4 GHz.

Temperature resistance of these materials was evaluated in an oven. The temperature was

progressively increased from 20 to 180 °C. Photographs were taken at each temperature level (Figure 4). Above 130 °C, the temperature becomes large enough to cause significant deformation and changes in the dimensions of the PLA-Fe load. At 150 °C, the PLA-Fe load is totally melted. In contrast, the PPS-Fe load shows no degradation up to 180 °C, in accordance with previous studies performed on the printable PPS matrix [19].

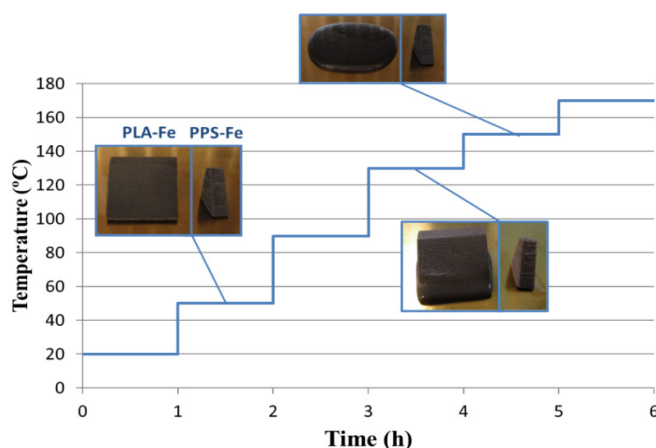


Figure 4. Heat treatment (20–180 °C) of PLA-Fe (left) and PPS-Fe (right) samples.

The power behavior of these components was evaluated using a test bench mainly consisting of a 30 W amplifier and a coupler (Figure 5). The directivity of the coupler is crucial since it ensures the isolation of the incident signal to the measurement port. The directivity of the selected coupler at 10 GHz (51.8 dB) makes it possible to maintain a difference of more than 30 dB between the leakage of the incident signal and the level of reflection of the load thus ensuring the validity of the measurements.

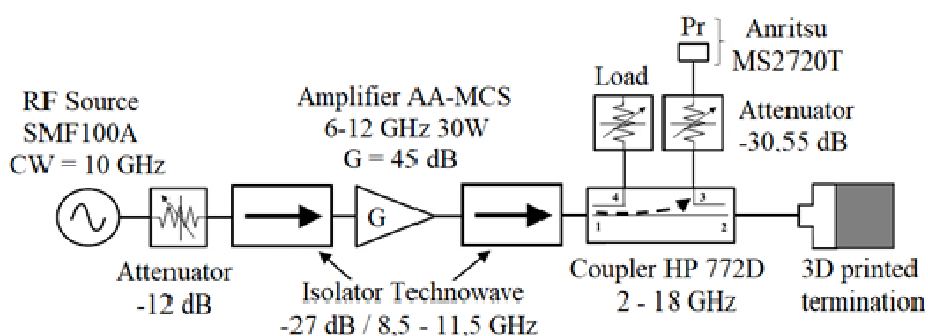


Figure 5. Test bench for the measurement of reflected power level as a function of incident power amplitude.

Figure 6 shows the evolution of the reflected power P_r as a function of the incident power P_{in} for pulses with duration of 10 s at 11 GHz. The measurement frequency was selected because of the highest directivity of the coupler at 11 GHz, thus ensuring the best accuracy of reflected power. One should note that, at this frequency, PLA-Fe load reflection coefficient is lower than the one of

PPS-Fe load. Up to 14.8 W, the PPS-Fe load has a constant reflection level highlighted by the linearity of P_r (P_{in}) with a slope corresponding to the reflection coefficient measured at low power level. Beyond this power level, the accumulation of heat in the absorber causes a local increase in temperature so that the component begins to melt. The maximum power level supported by PLA-Fe-based load is 4.8 W; namely a third of the PPS-Fe based load.

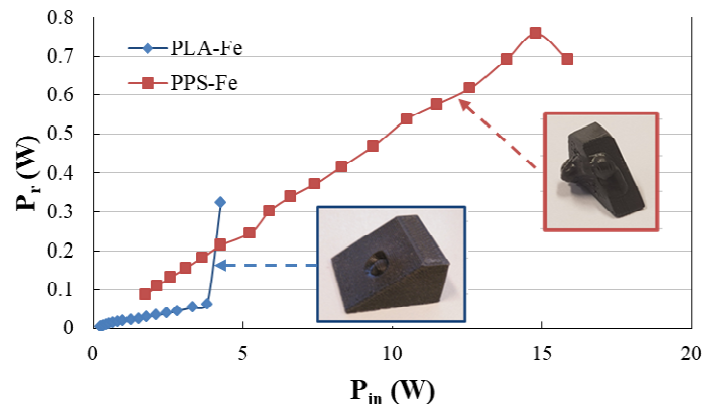


Figure 6. Reflected power as a function of the incident power for PPS-Fe (red square) and PLA-Fe (blue diamond) wedge loads at 10 GHz. Inserts: PLA-Fe load deteriorated beyond 4.8 W and PPS-Fe load deteriorated beyond 14.8 W.

A more efficient but longer PPS-Fe load was designed and fabricated to evaluate the thermal stability of EM properties. The dimensions of the load are the following: $l_b = 3$ mm, $l_p = 40$ mm and $w_p = 10$ mm. Then, reflection measurements were performed in a climatic chamber for temperature varying from -70 to 140 °C. Thru-Reflect-Line (TRL) calibration was performed at room temperature to remove the influence of the equipment used. Figure 7 shows that despite the temperature variation, the reflection coefficient remains below -24 dB throughout the frequency range. This result highlights the good temperature behavior of the printed PPS-Fe load.

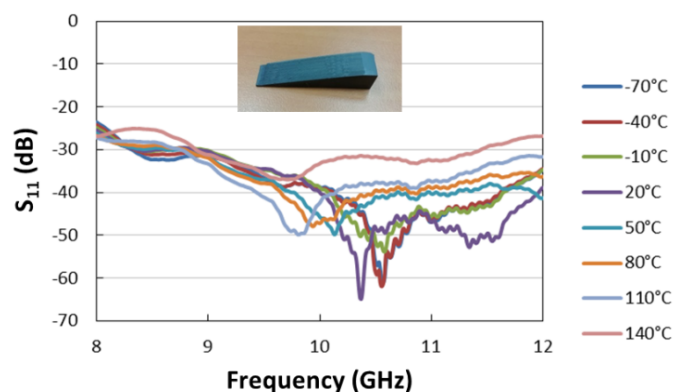


Figure 7. Amplitude of the reflection coefficient (S_{11}) of a PPS-Fe load in the 8–12 GHz frequency band for temperatures ranging from -70 to 140 °C.

These experimental results demonstrate that microwave loads with a high resistance to temperature and power can be realized by 3D-printing of a dedicated magnetic composite. For the moment, these demonstrations were performed on a simple 3D-printed absorbers inserted in a standard short-circuited metallic waveguide. However, we demonstrated earlier that the absorber can be printed together with its flange in order to get a low-cost low-weight component [11]. This approach will allow us achieving the fabrication, in a single process, of an efficient load compatible with harsh environment with a mass of a few grams that have to be compared with the mass of a standard X-band microwave load (between 50 and 200 g).

5. Conclusions

In this study, the printability of a PPS-Fe composite having a higher temperature resistance than the materials conventionally used in FDM 3D printing has been demonstrated. Two microwave loads in rectangular waveguide technology have been realized and characterized from this composite. PPS-Fe based load has a power handling greater than 14 W at 11 GHz, three times higher than a similar PLA-Fe load. Moreover, the return loss stability in the -70 to 140 °C temperature range is very promising with a return loss that is kept below -24 dB over the whole X-band in the temperature range. These results demonstrate that FDM technology can be used to design temperature and power resistant microwave absorbers.

The influence of the iron filling rates and particle sizes on the EM properties of the composite will be studied in the next step. In addition, our efforts will focus on the prediction of the power handling of the component through thermo-electromagnetic simulations.

Acknowledgments

This work was supported by the Centre National d'Etudes Spatiales (CNES) which is the government agency responsible for shaping and implementing France's space policy in Europe.

Conflict of interest

The authors declare no conflict of interest.

References

1. Chaidas D, Kechagias JD (2021) An investigation of PLA/W parts quality fabricated by FFF. *Mater Manuf Process* 1–9.
2. Spoerk M, Gonzalez-Gutierrez J, Sapkota J, et al. (2018) Effect of the printing bed temperature on the adhesion of parts produced by fused filament fabrication. *Plast Rubber Compos* 47: 17–24.
3. Mohan N, Senthil P, Vinodh S, et al. (2017) A review on composite materials and process parameters optimisation for the fused deposition modelling process. *Virtual Phys Prototy* 12: 47–59.

4. López AV, Rojas-Nastrucci EA, Córdoba-Erazo M, et al. (2015) Ka-band characterization and RF design of acrylonitrile butadiene styrene (ABS). *In To be presented in Microwave Symposium (IMS)*.
5. Tomassoni C, Bahr R, Tentzeris M, et al. (2016) 3D printed substrate integrated waveguide filters with locally controlled dielectric permittivity. *2016 46th European Microwave Conference (EuMC)* 253–256.
6. Lai W, Wang Y, He J (2020) Electromagnetic wave absorption properties of structural conductive ABS fabricated by fused deposition modeling. *Polymers* 12: 1217.
7. Kjelgard KG, Wisland DT, Lande TS (2018) 3D printed wideband microwave absorbers using composite graphite/PLA filament. *2018 48th European Microwave Conference (EuMC)* 859–862.
8. Ren J, Yin JY (2018) 3D-printed low-cost dielectric-resonator-based ultra-broadband microwave absorber using carbon-loaded acrylonitrile butadiene styrene polymer. *Materials* 11: 1249.
9. Laur V, Maalouf A, Chevalier A, et al. (2021) Three-dimensional printing of honeycomb microwave absorbers: Feasibility and innovative multiscale topologies. *IEEE T Electromagn C* 63: 390–397.
10. Lleshi X, Grelot R, Van Hoang TQ, et al. (2019) Wideband metal-dielectric multilayer microwave absorber based on a single step FDM process. *2019 49th European Microwave Conference (EuMC)* 678–681.
11. Arbaoui Y, Laur V, Maalouf A, et al. (2015) Full 3-D printed microwave termination: A simple and low-cost solution. *IEEE T Microw Theory* 64: 271–278.
12. Arbaoui Y, Laur V, Maalouf A, et al. (2015) 3D printing for microwave: Materials characterization and application in the field of absorbers. *2015 IEEE MTT-S International Microwave Symposium* 1–3.
13. Arbaoui Y, Agaciak P, Chevalier A, et al. (2017) 3D printed ferromagnetic composites for microwave applications. *J Mater Sci* 52: 4988–4996.
14. Omnexus, Glass Transition Temperature. Available from: <https://omnexus.specialchem.com/polymer-properties/properties/glass-transition-temperature#values>.
15. Wong KV, Hernandez A (2012) A review of additive manufacturing. *ISRN Mech Eng* 1: 1–10.
16. Wang X, Jiang M, Zhou Z, et al. (2017) 3D printing of polymer matrix composites: A review and prospective. *Compos Part B-Eng* 110: 442–458.
17. Espalin D, Muse DW, MacDonald E, et al. (2014) 3D printing multifunctionality: Structures with electronics. *Int J Adv Manuf Tech* 72: 963–978.
18. Sun XY, Cao LC, Ma HL, et al. (2017) Experimental analysis of high temperature PEEK materials on 3D printing test. *2017 9th International conference on measuring technology and mechatronics automation (ICMTMA)* 13–16.
19. Laur V, Abboud MK, Maalouf A (2018) Heat-resistant 3D printed microwave devices. *2018 Asia-Pacific Microwave Conference (APMC)* 1318–1320.

